AIAA JOURNAL
Vol. 36, No. 4, April 1998

Measurement of Three-Dimensional Crossflow Separation

Todd G. Wetzel,* Roger L. Simpson,† and Christopher J. Chesnakas‡
Virginia Polytechnic Institute and State University, Blacksburg, Virginia 24061

Parameters and techniques for detecting the location of three-dimensional crossflow separations are evaluated using several data sets. Several definitions of separations and the physics of the separation process are discussed along with descriptions of the separated flowfield. Measurement techniques that depend on each of these descriptions are then considered, and data are compared and contrasted. The data analyzed here represent a very rare combination of many different measurement techniques applied to the same geometry and apparatus from several different studies, including oil flow visualization, laser Doppler velocimetry, surface pressure, and surface hot-film skin-friction measurements (magnitude only and directional). Pressure is the least sensitive of the indicators of separation, although minima in rms pressure fluctuations correlate well with separation location. Hot-film skin-friction magnitude measurement is one of the easiest and most accurate techniques; local minima correlate well with separation location. Laser Doppler velocimeter measurements provide the most detail about the separation flowfield but at great expense and with the limitation of requiring knowledge of the separation line direction. Directional surface hot-film measurements provide data that, when integrated, yield a global measurement of separation and detailed surface topology. The issues discussed in this work are also relevant when interrogating computational fluid dynamics data sets for separation phenomena.

Nomenclature

C_f	= skin-friction coefficient, τ_w/q_∞
Cf_{lat}	= component of C_f perpendicular to body axis
Cf_{long}	= component of C_f parallel to body axis
Cp	= surface pressure coefficient, $(p - p_s)/q_\infty$
Cp_{rms}	= root mean square of surface pressure coefficient
L	= model length
p	= pressure
p_s	= static pressure
q_∞	= upstream dynamic pressure, $\frac{1}{2}\rho U_\infty^2$
Re	= Reynolds number, $U_\infty L/\nu$
r	= radial distance from model surface
U	= local streamwise velocity
U_∞	= freestream velocity
V	= wall-normal velocity
W	= crossflow velocity
W_s	= crossflow velocity perpendicular to separation line
x	= model longitudinal position from nose
y	= wall-normal coordinate
α	= angle of attack
δ_{1R}	= displacement thickness
μ	= viscosity
ρ	= air density
τ_w	= wall shear
χ	= circumferential coordinate, deg

I. Introduction

FLOW separation from a body surface plays a dominant role in the aerodynamic performance of many systems. The mere detection of the existence of separation can be adequate for many engineering problems. As a result, especially in three-dimensional flows, the definition of separation is rarely addressed rigorously. The comparison of the separation locations of two similar flows illustrates the importance of fine measurement resolution near separation. This requires careful consideration of the definition of separation and the precision of the measurement technique used.

Several researchers discuss the qualitative nature of separation. Simpson[1] discusses various traits of three-dimensional turbulent separation, whereas Tobak and Peake[2] have written a description of three-dimensional flow separation topology and Yates and Chapman[3] have discussed the related separation kinematics. No definitive work exists, however, on the precise measurement of three-dimensional crossflow separation. Such is the purpose of this paper.

II. Separation Definition

The separations that typically form on bodies at angles of attack are called crossflow separations due to the dominance of the circumferential pressure gradients in the separation process. These separations typically develop from the rear of the body at very low angles of attack and stretch forward at increasing angles of attack. In the simplest case, the crossflow separation is delineated by the primary separation line. In regions where the separation is strong, a separation sheet rolls up into a vortex (Fig. 1). In stronger separations, secondary vortices can form.

A. Start of Crossflow Separation

Crossflow separations are characterized as open separations because the separation line has a free endpoint on the model surface. Yates and Chapman[3] state that, although many types of separations (global separations) have specific singularities on the surface as a starting point, crossflow separations represent a special case (local separations) that do not originate from a unique singularity but instead, like all surface streamlines, originate from the stagnation point. Interestingly, because open separations are characterized by the convergence of many streamlines, Yates and Chapman state that there is no unique separation line. Han and Patel's[4] experimental work, along with the work of the present authors, supports this fact. Practically speaking, it seems reasonable that one should be able to create a definition for the start of separation. Yates and Chapman note that on the nose of a body of revolution at incidence the flow is fully attached, whereas the flow at the tail exhibits all of the characteristics of a strong separation. It therefore seems reasonable that a practical start of separation must exist where the separation has some measurable presence, though this point is not the separation origination.

Efforts to define such a practical criterion have so far proved fruitless. Few detailed measurements have been made in the vicinity of

Received Feb. 18, 1997; revision received Dec. 18, 1997; accepted for publication Dec. 22, 1997.

*Research Associate, Department of Aerospace and Ocean Engineering; currently Heat Transfer Engineer, General Electric Corporate R&D Center, Schenectady, NY 12301. Member AIAA.

†Jack E. Cowling Professor, Department of Aerospace and Ocean Engineering. Fellow AIAA.

‡Research Associate, Department of Aerospace and Ocean Engineering; currently Mechanical Engineer, Carderock Division, Code 5400, David Taylor Model Basin, U.S. Naval Surface Warfare Center, 9500 MacArthur Boulevard, West Bethesda, MD 20817-5700. Member AIAA.

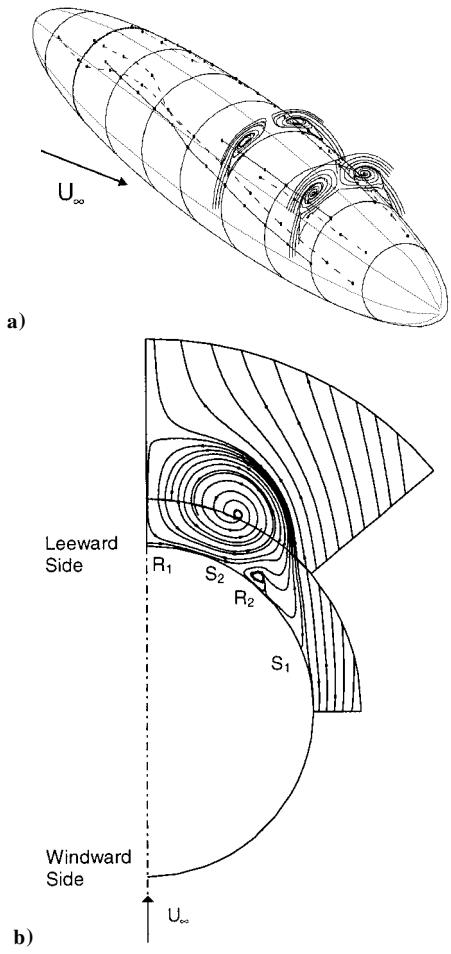

Fig. 1 Simplified crossflow separation topology for a 6:1 prolate spheroid, α = 20 deg and Re = 4.2 × 10^6: a) three-dimensional view: ——, oil flow separation locations; – – –, skin friction minima; secondary flows are drawn at x/L = 0.60 and 0.77; and b) frontal view of secondary flow streamlines for x/L = 0.77 location in local model surface coordinates: S_1 and S_2 are primary and secondary separation locations, respectively, and R_1 and R_2 are primary and secondary reattachment locations.[8,12]

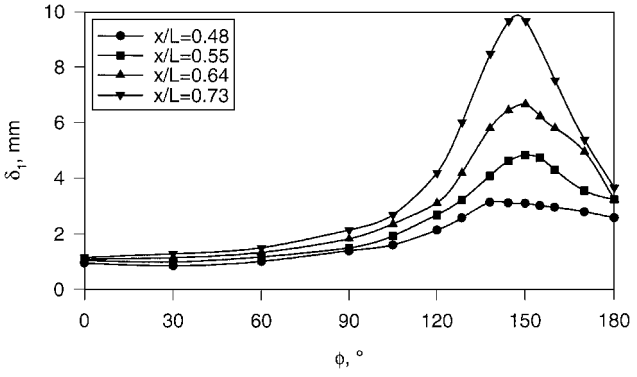

Fig. 2 Development of three-dimensional boundary-layer displacement thickness at Re = 7.7 × 10^6 on a 6:1 prolate spheroid at α = 10 deg for several axial locations.[5]

the start of a crossflow separation to provide evidence for the existence of a practical starting location. All indicators proceed gradually from an unseparated condition to a separated one. For example, the displacement thickness data[5] in Fig. 2 for a prolate spheroid at α = 10 deg show that δ_{1R} grows gradually without any indication of where a separation might begin.

It is arguable whether the start of separation is important to find. The flow near a hypothetical start of crossflow separation is very nearly attached and, thus, does not significantly interact with the freestream. Any separation that is too weak to measure with conventional sensors is also too weak to have a significant effect on the local flowfield.

The nonuniqueness of a crossflow separation is a very important trait. However, in regions of significant separated flow, there exist topological features that are identifiable to a lesser degree of rigor. Therefore, although there may be no unique separation line in the purest sense, for example, there does exist an identifiable topological feature that behaves in many ways like a distinct separation line. Therefore, in the discussions that follow, references to the separation line or other ideally distinct features are not meant to ignore the nonuniqueness of crossflow separation but instead are meant to acknowledge the practical and necessary framework within which real separations can be analyzed.

B. Identifying Traits of Crossflow Separation

For weak or beginning separations, crossflow separation lines form due to a significant thickening of the leeward shear layer and the formation of a sheet of fluid that exhibits relatively large wall-normal velocity components.[1] This separation sheet has one edge coincident with the separation line and is an interface between windward side and leeside flows. Because this separation, both as a sheet in the flow and as a line on the model surface, is a real boundary, no fluid can pass through it. Thus, streamlines on either side of a separation converge asymptotically toward the separation sheet/line. There is a significant velocity component tangent to this line resulting in nonzero skin friction. However, it is the relatively large wall-normal velocities that characterize an uplifted region of flow as separated.[1] The fundamental effect that differentiates true separation from mere thickening of the shear layer is a substantial interaction between the fluid leaving the model via the separation and the inviscid external flow.[1] The important side effect of separation and thus its defining trait is the breakdown of normal boundary-layer flow, resulting in the significant departure of fluid away from the body surface and creating regions of converging flow on opposite sides of separation.[1]

It can be shown that these large wall-normal velocities are indirectly related to wall shear. By analyzing the continuity and momentum equations near the wall, it can be shown that[6]

$$V = -(1/2\mu)(\nabla \cdot \boldsymbol{\tau}_w)y^2 + (1/6\mu)(\nabla^2 p)y^3 + \cdots$$

Thus, wall shear is a lower-order indicator of wall-normal velocity than pressure. To use this equation rigorously, the entire wall shear vector field would need to be known to perform the divergence operation. It will be shown that, in practice, crossflow separations occur very near wall shear stress magnitude minima.

More can be learned about the contributing physics of these skin-friction trends by examining the directional skin-friction data of Kreplin et al.[7] Figure 3 shows the circumferential distribution of the components of the skin friction for a 6:1 prolate spheroid at α = 30 deg. As would be expected, the component of skin friction in the crossflow direction (Cf_{lat}, in the same direction as the W velocity component) is nearly zero at separation. These data are presented in a body surface coordinate system and not a coordinate system

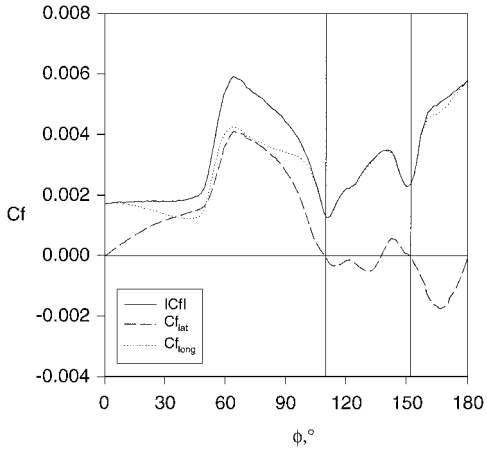

Fig. 3 Circumferential distributions of skin-friction magnitude and components at x/L = 0.738 on a 6:1 prolate spheroid at α = 30 deg and Re = 6.5 × 10^6; vertical line indicates where separations were found from integrating the directional skin-friction field.[7]

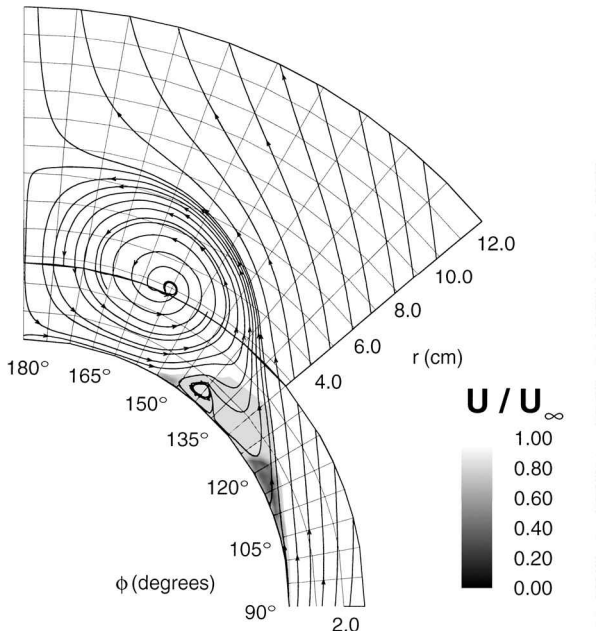

Fig. 4 Total velocity contours and secondary streamlines in body surface coordinates at α = 20 deg and x/L = 0.77 for a 6:1 prolate spheroid; notice low-momentum fluid leeward of apparent primary separation. Model diameter at this location is 19.24 cm (Ref. 8).

perpendicular to the separation line. Therefore, Cf_{lat} should not be exactly zero at separation. The minimum in the total skin-friction magnitude corresponds to the minimum in the component of skin friction parallel to the model axis (Cf_{long}), which in turn indicates a localized minimum in the U velocity component (parallel to the model axis) near the wall. Chesnakas and Simpson[8] have identified such a minimum in total velocity in the laser Doppler velocimetry (LDV) measurements shown in Fig. 4. In this coordinate system the secondary flow streamlines appear to indicate a low-velocity trough on the lee side of separation. The results in this paper, when presented in a coordinate system aligned with the separation line, will show that this low-velocity trough is located directly at separation.

III. Measurement Techniques and Their Separation Descriptions

Several different measurement techniques are used as indicators of features of separation. Each technique is now discussed in terms of a specific separation descriptor.

A. Converging Skin-Friction Lines

1. Oil Flow Visualization

Pigment streaks in the oil flow pattern indicate surface skin-friction directions. Figure 5 shows an example of an oil flow on a 6:1 prolate spheroid. In strongly separated flows, separation lines are easy to distinguish, as are other flow topologies. Separation initiation is difficult to pinpoint, and separation lines in weakly separated flows are also difficult to discern. Meier and Kreplin[9] have shown that the oil flow tends to indicate separation too far windward, and this is strongly supported by comparisons with hot-film data later in this paper. The errors can be attributed to gravity effects or direct interactions between the flowfield and the oil mixture, which tends to pool near separations.[10] Oil flows can also influence transition and, thus, transition-sensitive separations. These errors can be very significant, and so oil flows should be used for qualitative interpretations of the flow only.

2. Surface Skin-Friction Vectors via Directionally Sensitive Hot-Film Sensors

Measurements of the surface skin-friction direction, such as those performed by Kreplin et al.,[7] provide perhaps the most direct way of measuring the separation topology. The sensors rely only on a relationship between heat transfer and skin friction, which tends to be at least monotonic, and in practice are accurate to within 5% in relative magnitude and 10% in direction.[7] Errors due to heating the fluid are assumed to be negligible the rapid mixing associated with both turbulent boundary layers and separated flows. Measurements in one cross section are not adequate for precisely locating separation unless the local direction of the separation line is already known. Instead, the global field of measured skin-friction magnitudes and directions must be integrated to obtain the surface streamlines.

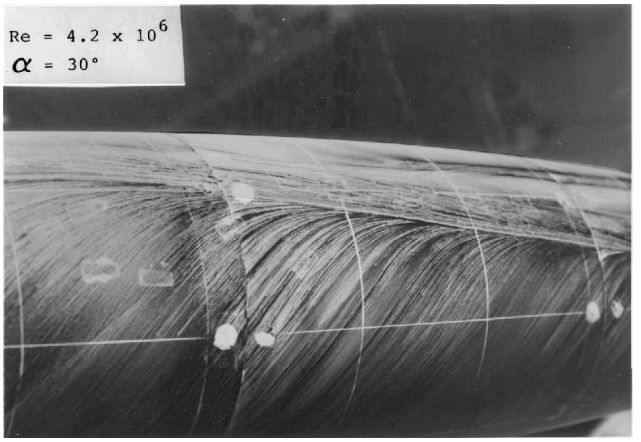

Fig. 5 Oil flow over the leeside tail of an untripped 6:1 prolate spheroid; flow is from left to right.

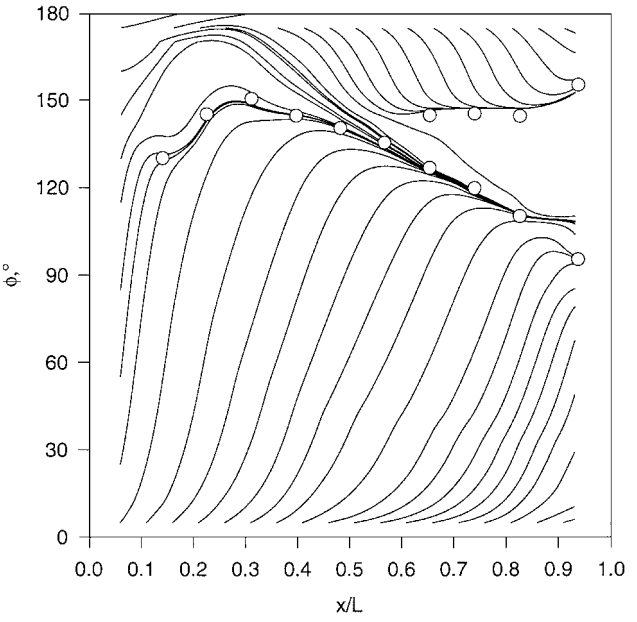

Fig. 6 Typical skin-friction streamline pattern obtained from directional hot-film skin-friction gauges on a 6:1 prolate spheroid[7]: ∘, local skin-friction magnitude minima; $Re = 6.5 \times 10^6$; and α = 20 deg.

An example of this is presented in Fig. 6. The separation definition used is rigorous, and the technique has no inherent biases. Limitations result from measurement uncertainties and spatial resolution, both of which are difficult to assess. One can readily see an error near the tail in Fig. 6, where the separation line turns to a constant χ instead of a continued sloping to the windward. The current authors perturbed the data of Ref. 7 by up to a 10% error (both randomly and with a bias) and found that the errors were significant only at lower angles of attack (~10 deg), where the separations are weaker, form more gradually, and are in general more uncertain. An advantage of the directional skin-friction technique is that no magnitude calibration is required of the sensors, but directional calibration is necessary.

B. Local Crossflow Velocity W Nearest the Wall Is Zero

Zero crossflow velocity as a separation indicator is used because the surface separation line is a limiting streamline, and as such the

crossflow velocity perpendicular to it must be zero. This is identical to examining a secondary flow streamline pattern in a separated region and searching for the one secondary flow streamline that leaves perpendicular to the model surface. However, the location of this secondary flow streamline is dependent on the coordinate system. This is because, of course, the crossflow velocity of all streamlines, in a coordinate system tangent to the streamline, is zero. It is true that crossflow separation lines are often roughly parallel to the body axis, but to be precise the velocity data must be transformed to a coordinate system that is locally tangent to the separation line. Therefore, global data are required to know the separation line direction.

LDV, such as used by Chesnakas and Simpson,[8,11] is presently the only practical technology for making accurate near-wall, three-velocity-component measurements, with typical uncertainties of 1% of freestream velocity or better. The measurements must be made very close to the wall where the separation sheet is still normal to the model surface. The separation sheet skews leeward very rapidly as one traverses through the boundary layer. Usually hot wires cannot get close enough to the wall. However, because the crossflow velocity is identically zero on the wall at all locations, measurements must be made far enough away from the wall to decrease uncertainties.

An example of this type of data is shown in Fig. 7. Here, the data of Chesnakas and Simpson[8] at $x/L = 0.77$ and $\alpha = 10$ deg have been interpolated to obtain circumferential distributions of crossflow velocity W at various fixed radii away from the model. The crossflow velocity W is in a body-axis coordinate system. The point where W is zero closest to the wall is the apparent separation location. At the farthest radii shown, the crossflow velocity is zero at around 150 deg, but as one moves toward the wall, that crossing point moves windward until it seems to converge at around 123 deg.

However, this crossflow velocity is not exactly perpendicular to the separation line location. Using oil flows to obtain the approximate local separation line direction, the velocities of Chesnakas and Simpson[8] were transformed to a coordinate system perpendicular to the separation line. Figure 8 shows the resultant crossflow velocity W_s distributions. The separation line, now more accurately defined, has moved leeward by 20 deg to $\chi = 143$ deg. In regions of weak separation, the slope of the W–χ curve close to the wall is very small, and the U velocity is typically larger than W. Therefore, small coordinate rotations can result in large movements of the indicated separation line. In this case, a coordinate rotation of 8.5 deg (determined from oil flows) moved the apparent separation line 20 deg circumferentially. It is also important to point out that it can be difficult to determine this coordinate rotation with precision. In this case, the 8.5-deg rotation is accurate only to within ± 1 deg, so that the corrected separation location also has a relatively high uncertainty.

C. Wall-Normal Velocity V Is Maximum near Separation

This argument is based on a more fundamental description of separation as the significant departure of fluid away from the body.

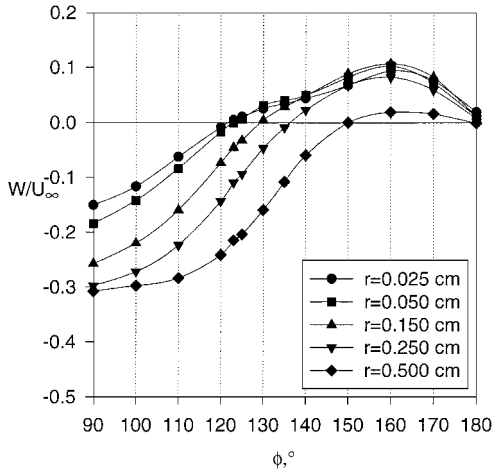

Fig. 7 Circumferential distributions of crossflow velocity at fixed distances from model surface, $\alpha = 10$ deg, $x/L = 0.77$, and $Re = 4.2 \times 10^6$; crossflow velocity in body surface coordinates.[8,12]

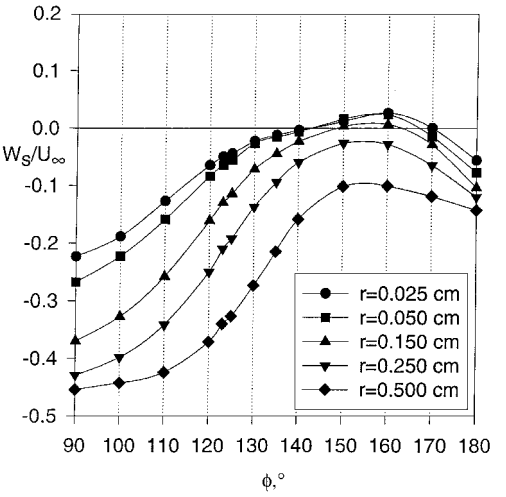

Fig. 8 Circumferential distributions of crossflow velocity at fixed distances from model surface, $\alpha = 10$ deg, $x/L = 0.77$, and $Re = 4.2 \times 10^6$; crossflow velocity in coordinate system perpendicular to local separation line.[8,12]

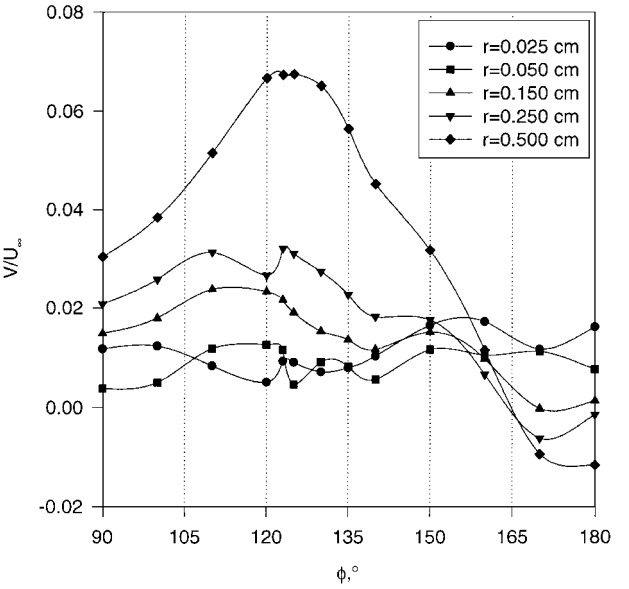

Fig. 9 Circumferential distributions of wall-normal velocity at fixed distances from model surface, $\alpha = 10$ deg, $x/L = 0.77$, and $Re = 4.2 \times 10^6$; model diameter at this location is 19.24 cm (Refs. 8 and 12).

Tobak and Peake[2] show that converging streamlines on each side of a separation by necessity result in a locally large wall-normal velocity component at separation. However, there is no requirement for the largest wall-normal velocity component to correspond exactly to the separation location. The separation sheet is perpendicular to the model surface, but it quickly skews leeward away from the model surface.

Again, LDV gives a direct measure of these near-wall velocities. The only further advantage is that no information about the separation line direction is needed so long as the coordinate system chosen is normal to the model surface. Figure 9 shows data from Chesnakas and Simpson[8] for $\alpha = 10$ deg and $x/L = 0.77$. Far away from the wall, large positive (outward) normal velocities exist, but they are windward of separation. Closer to the wall, where the maximum will more accurately determine separation location, the scatter in the data due to measurement uncertainties of the near-zero velocities makes resolution of a maximum very uncertain. Whereas a locally large wall-normal velocity represents a necessary condition for separation, it does not serve as a practical separation indicator.

D. Skin-Friction Magnitude Is Minimum near Separation

Surface skin-friction magnitude can be measured by directionally insensitive hot-film sensors. This is perhaps the easiest technique of

all, as it requires the fewest measurements. Hot-film sensors heat the near-wall fluid through forced convection. Because of the similarity between gradient transport of momentum and scalars (heat), the amount of heat transfer into the fluid gives a measure of the wall shear. The main purpose of these sensors is not necessarily to measure the true magnitude of the skin-friction coefficient but to measure the relative shear distributions and, thus, the locations of wall shear minima. Wall shear magnitudes are possible with proper calibration, though this is difficult in practice.

A minimum in wall shear magnitude is assumed to be an indication of the local maximum near-wall normal velocity component, which is in turn interpreted to be the separation location. Therefore, wall shear minimum is not a rigorous separation definition, but in practice it works quite well as shown by the skin-friction data of Kreplin et al.[7] in Fig. 6. (The stated skin-friction uncertainty is $\pm 10\%$.) The circles represent locations of local wall shear minima, and they correspond to the separation locations to within uncertainties.

Especially in weak separations, the wall-shear minima can be fairly shallow. When this flatness is coupled with noise in the data, the precise determination of the minimum location can be difficult. Curve fitting has not worked due to the typical asymmetry of the wall shear distribution surrounding a minimum.[12] In Ref. 12, the data surrounding the minimum were smoothed with a Loess smoothing technique, and the resultant minimum was selected automatically by the host computer. This process provided a consistent algorithm for selecting the minimum location from real wall shear data.[12] The relative uncertainties of these measurements are $\pm 5\%$.

Figure 10 shows the circumferential distribution of skin-friction magnitude at $x/L = 0.729$ on a prolate spheroid at various α. At low angles of attack, there is a minimum indicating separation. At 20-deg angle of attack and above, the second valley indicates the presence of a secondary separation. The symbols representing primary separations from the oil flows show the large windward bias of the oil flow separation data. In practice, the oil flow separation location is bounded by the skin-friction magnitude minima on the leeside and the minima in the crossflow skin friction gradient ($\partial Cf/\partial\chi$) on the windward side.

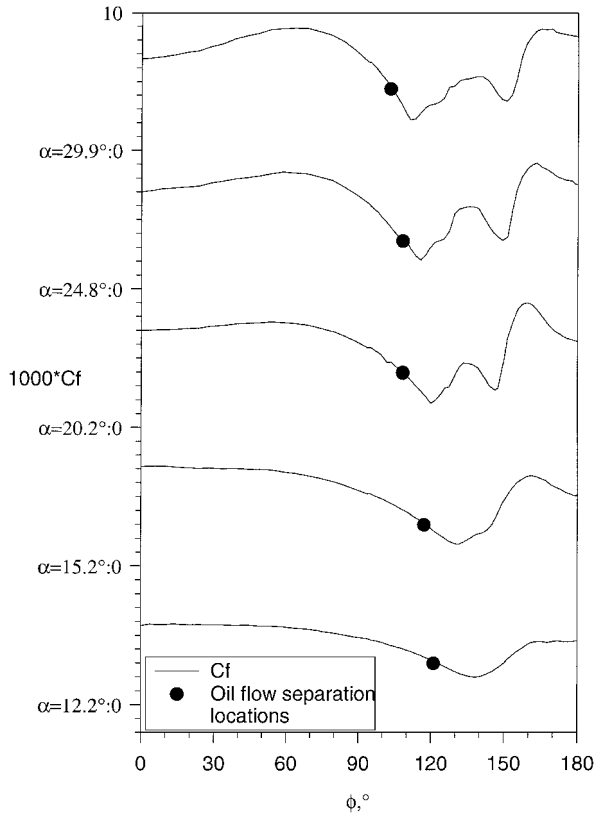

Fig. 10 Circumferential distributions of skin-friction magnitude at $x/L = 0.729$ on a 6:1 prolate spheroid at various angles of attack, $Re = 4.2 \times 10^6$ (Ref. 12). Note offset ordinates.

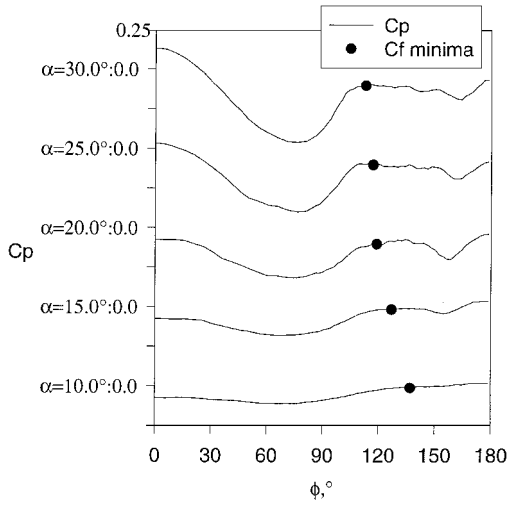

Fig. 11 Circumferential pressure distributions at $x/L = 0.77$ on a 6:1 prolate spheroid at various angles of attack, $Re = 4.2 \times 10^6$ (Ref. 12). Note offset ordinates.

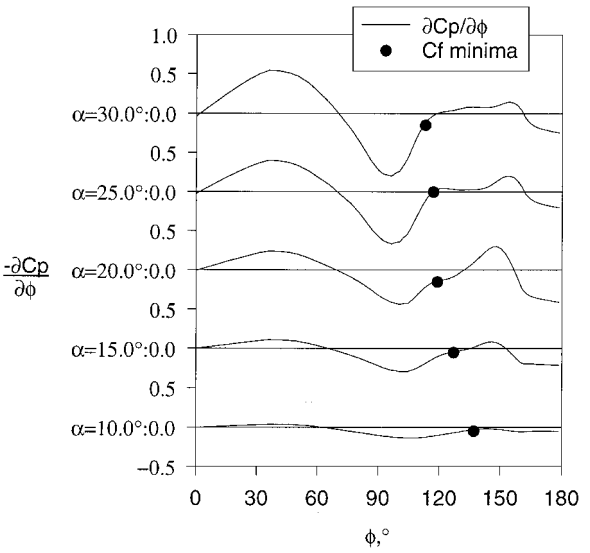

Fig. 12 Circumferential pressure coefficient gradient (1/rad) distributions at $x/L = 0.77$ on a 6:1 prolate spheroid at various angles of attack, $Re = 4.2 \times 10^6$ (Ref. 12).

E. Separation Results in Changes in Surface Pressure

1. Mean Surface Pressure and Crossflow Pressure Gradient

Pressure data are often used to indicate the existence of massive separation but do not indicate the separation location well. The reason pressure is not a good indicator of the location of a local phenomenon is that the pressure at a given point in space is strongly influenced by the entire flowfield.[13] The works of Poll[14] and Hall[15] on ogive cylinders, Chang and Purtell[16] on submarine-like bodies of revolution, and the current authors on prolate spheroids show conclusively that pressure distributions give very weak indications of the location of separation. Figure 11 shows plots of circumferential pressure distribution at $x/L = 0.77$ on a prolate spheroid at various α. The uncertainties in these data are $\pm 10\%$. The pressure distribution is flat in regions of separation, and this again is qualitatively true. However, it is difficult to pinpoint a location where this flat pressure distribution begins. Chang and Purtell[16] list the very simple model Tinker[17] used for determining the location of separation as 15 deg leeward of the minima in pressure magnitude. The data in Fig. 11 show separation farther leeward of this point. The peripheral pressure gradient shown in Fig. 12 also has a local minimum much more windward of the separation.

2. Pressure Fluctuations

Figure 13 shows the circumferential distribution of rms surface pressure fluctuations from the work of Goody et al.[18] for the same

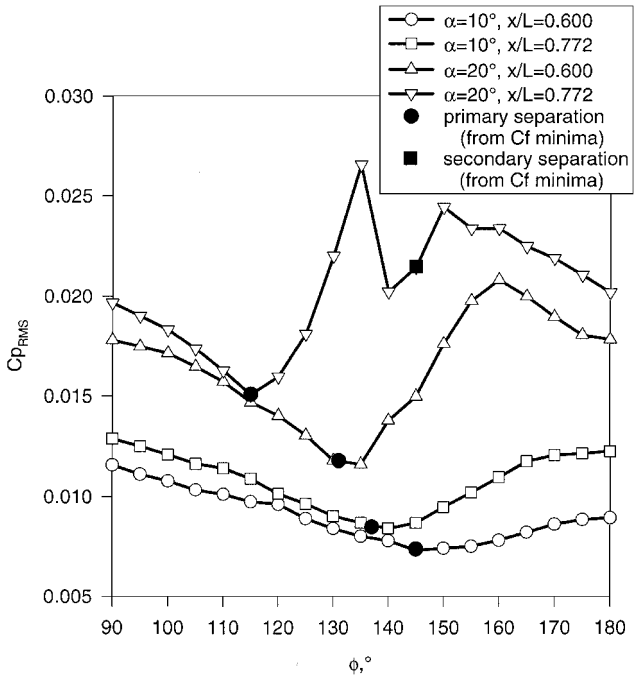

Fig. 13 Circumferential distributions of rms pressure fluctuations on a 6:1 prolate spheroid, $Re = 4.2 \times 10^6$ (Ref. 18). Distributions are successively offset vertically by 0.002 for clarity.

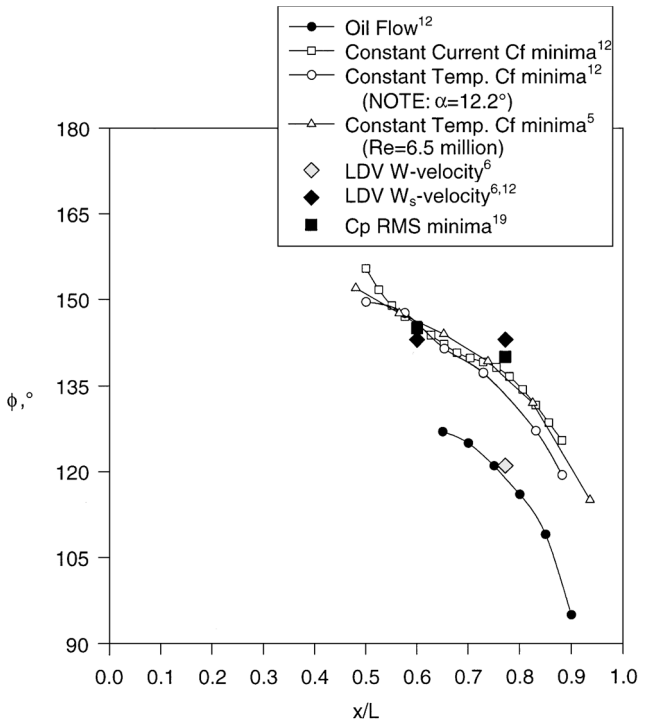

Fig. 14 Various primary separation line comparisons for $\alpha = 10$ deg and $Re = 4.2 \times 10^6$.

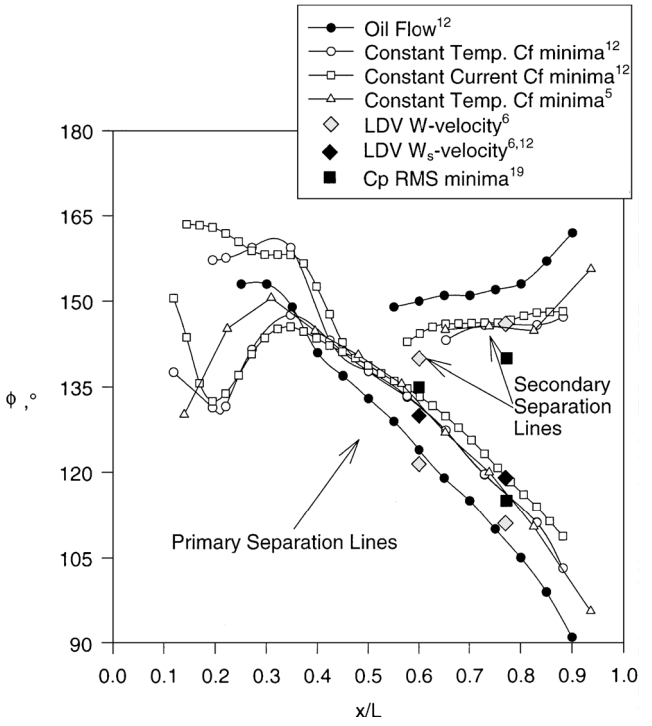

Fig. 15 Various primary and secondary separation line comparisons for $\alpha = 20$ deg and $Re = 4.2 \times 10^6$.

model and flow conditions as for the oil flow, LDV, and skin-friction data. These rms pressure fluctuations were calculated after adjusting the spectra for nonturbulence noise sources (facility acoustic signature, etc.), the transfer function of the pressure transducer, and the unmeasured high-frequency contributions to the rms value; they have a stated uncertainty of ±1.5%. These data indicate that the pressure fluctuations seem to reach a minimum very near separation. These pressure measurements were taken every 5 deg circumferentially. Perhaps a tighter measurement grid would yield even better correlation with the separation locations.

The regions of low surface pressure fluctuations are directly below regions with low turbulent kinetic energy.[18] It is believed that windward of separation the growing turbulent boundary layer produces increasing pressure fluctuations. The large outflow associated with separation transports turbulent energy away from the near-wall region near separation, leading to a reduction in pressure fluctuations as separation is approached. Leeward of separation, the large vortical separated flowfield produces very large turbulent structures, leading to increased values of pressure fluctuations. Separation is not rigorously located by minima in pressure fluctuations, but this does seem to be as good an indirect indicator as skin-friction magnitude. Surface pressure fluctuation rms values are difficult to measure with precision in practice due to the complicated correction issues, very wide frequency requirements, and the large data sets necessary for good statistics.

F. Separation Line Comparisons from Different Measurement Techniques

Figures 14 and 15 show a comparison of the separation lines on a 6:1 prolate spheroid for $\alpha = 10$ and 20 deg, respectively. Data are taken from the oil flow data and magnitude hot-film (constant current and constant temperature) data of Wetzel,[12] the directional hot-film data of Kreplin et al.,[7] the LDV data of Chesnakas and Simpson,[8,11] and the pressure fluctuation data of Goody et al.[18] For the LDV data, the separation locations were selected using the W and W_s plots as in Figs. 7 and 8. The models in all studies had boundary-layer trip strips at $x/L = 0.20$.

In all cases, the oil flows indicate separation windward of the skin-friction minima. At $\alpha = 10$ deg, the constant current data and Kreplin et al.[7] data (despite being at a larger Reynolds number) all agree very well. Ahn and Simpson[19] have shown that the crossflow separation on the tail of a prolate spheroid is very insensitive to Reynolds numbers above 2.6×10^6. The constant temperature data of Wetzel[12] are slightly windward because they were taken at a slightly higher angle of attack (12.2 deg). At $\alpha = 10$ deg and $x/L = 0.77$, the LDV separation determined from a body coordinate system is about 15 deg windward of the skin-friction minima. Transforming the velocity data parallel to the separation line moves the LDV separation location 20 deg leeward to roughly $\chi = 143$ deg. This correction is in the proper direction but is roughly 5 deg leeward of the skin-friction minimum due to uncertainties in the 8.5 ± 1 deg angle of the separation line. Pressure fluctuation minima are very close to separation locations and would probably correlate better had data been obtained on a tighter grid spacing.

At $\alpha = 20$ deg (Fig. 15), the oil flow is again windward of the wall shear minima. The unrotated LDV data show zero W consistently windward of the wall shear minima, but the rotation transformation moves the LDV primary separation lines to near-perfect correlation with the wall shear minima. The secondary separation LDV locations were not transformed because the secondary separation is very closely aligned with the body axis. The pressure minima correlate well with the primary separation given the 5-deg spacing of the data but correlate poorly with the secondary separation. The poor agreement between pressure minima and secondary separation may be due to significantly higher uncertainties in the pressure data within the separated region.

G. Local vs Global Data

A general conclusion in examining these three-dimensional data sets is the distinction between local and global measurement requirements. In general, any method that locates a flow topology using directionally biased assumptions will be locally inaccurate unless global information is obtained. The clearest example of this effect is the use of the LDV crossflow velocity measurements, which when used by themselves in body coordinates can result in separation location errors of as much as 15 deg around the body; when the data are corrected using the local direction of the separation line, the separation locations become more accurate. This method is in contrast to local measurement techniques, such as skin-friction magnitude, which are independent of coordinate system.

One must recognize that this dependence on coordinate system for locating flow topologies accurately cannot be understated and applies to all flowfield topologies, not just separation locations. A flow topology is a shape or structure delineated by flow pathlines, which are defined by flow velocities. Searching for the accurate location of a topology is based on some description in terms of velocity. The accuracy of that search is then dependent on the coordinate system in which the flow velocities are based.

One additional example of the impact of coordinate system on topology location is the determination of the location of a vortex center in three-dimensional space, such as the separated vortices that form due to a crossflow separation. Yates and Chapman[3] define the center of a vortex as the streamline with locally minimum curvature in space. To determine the curvature of a streamline in space, global data are required. It is more common instead for researchers to make measurements in a plane and construct the secondary flow streamlines as a means of determining the vortex center (for example, Fig. 4). Presumably, this would be the location of zero V and W velocity. However, if the coordinate system is not locally perpendicular to the vortex, this point of zero V and W velocity is not the vortex center.

H. Application to Computational Data Sets

Separation locations require the interpretation of some fundamental flow quantity, such as velocity, skin friction, pressure, etc. Likewise, separation locations are not directly computed in a computational fluid dynamics (CFD) calculation. The user of any CFD code must interpret the fundamental flow quantities in an identical fashion as an experimentalist when searching for precise separation locations. All of the experimental issues discussed here have either direct parallels or analogies in interpreting computational data. As one example, one cannot find separation by examining secondary flow streamlines unless it is known that those secondary flow streamlines are represented in a coordinate system that is oriented with the local separation line direction. As an additional example, a CFD user may have a difficult time using wall-normal velocities as a direct indication of separation due to the large ratio of roundoff errors or numerical noise (paralleling experimental uncertainties and noise) relative to the near-zero velocities close to the wall.

IV. Conclusions

Three-dimensional crossflow separation was discussed, and several flow quantities that are used for separation detection were examined. Oil flows are very commonly used to indicate separation topologies but can indicate separations that are too windward and should be used for qualitative separation measurements only. LDV for three velocity components is the most detailed technique but also the most complicated, time consuming, and expensive. Also, the requirement to measure very near the wall results in high-percentage uncertainties as the velocity approaches zero. Finally, it is clear that the apparent separation locations obtained from this technique can be in error without knowledge of the local separation direction a priori. These limitations also apply to other velocity measurement techniques.

The hot-film magnitude data present the easiest technique but require a tight grid and low data scatter to resolve precise minima. The directional skin-friction data provide a high level of detail so long as data are obtained globally. The directional sensors also require twice the effort of the nondirectional gauge for the same number of measurement locations but may not require as tight a grid as the magnitude-only measurements. It is unclear quantitatively how numerical uncertainties in the directional measurements impact the separation location in such a technique, although it is known that uncertainties affect low-angle-of-attack data (or weak separations) most significantly. Whereas these data would make possible plots such as those of Fig. 6, there remains the problem of algorithmically extracting the separation lines from the other skin-friction lines.

Mean pressure data and mean circumferential pressure gradients are not good separation indicators, but surface pressure fluctuation minima are. In general, any criterion for locating a flow topology that uses directionally biased data requires global information to be used with precision. All of the issues raised with regard to precisely locating separation location from experiments apply to the interrogation of CFD results as well.

Acknowledgments

The authors are grateful for support by Office of Naval Research (ONR) Contracts N00014-91-J-1732 and N00014-95-I-0101 for hot-film measurements and for the years of encouragement by James A. Fein, Program Manager. The laser Doppler velocimetry work was supported by ONR Contract N00014-94-1-0092, L. P. Purtell, Program Manager. The oil flow photograph was taken by Jennifer Krahulec.

References

[1] Simpson, R. L., "Aspects of Turbulent Boundary Layer Separation," *Progress in Aerospace Sciences*, Vol. 32, Nov. 1996, pp. 457–521.

[2] Tobak, M., and Peake, D. J., "Topology of Three-Dimensional Separated Flows," *Annual Review of Fluid Mechanics*, Vol. 14, 1982, pp. 61–85.

[3] Yates, L. A., and Chapman, G. T., "Streamlines, Vorticity Lines, and Vortices Around Three-Dimensional Bodies," *AIAA Journal*, Vol. 30, No. 7, 1992, pp. 1819–1826.

[4] Han, T., and Patel, V. C., "Flow Separation on a Spheroid at Incidence," *Journal of Fluid Mechanics*, Vol. 92, Pt. 4, 1979, pp. 643–657.

[5] Kreplin, H. P., and Stäger, R., "Measurements of the Reynolds-Stress Tensor in the Three-Dimensional Boundary Layer of an Inclined Body of Revolution," *Ninth Symposium on Turbulent Shear Flows*, Dept. of Mechanical Engineering, Kyoto Univ., Kyoto, Japan, 1993, pp. 2-4-1–2-4-6.

[6] Vollmers, H., Kreplin, H. P., and Meier, H. U., "Separation and Vortical-Type Flow Around a Prolate Spheroid—Evaluation of Relevant Parameters," AGARD CP-342, Paper 14, 1983, pp. 14-1–14-14.

[7] Kreplin, H. P., Vollmers, H., and Meier, H. U., "Shear Stress Measurements on an Inclined Prolate Spheroid in the DFVLR 3 m × 3 m Low Speed Wind Tunnel, Göttingen—Data Report," DFVLR Rept. IB 222-84 A 33, Jan. 1985.

[8] Chesnakas, C. J., and Simpson, R. L., "Detailed Investigation of the Three-Dimensional Separation About a Prolate Spheroid," *AIAA Journal*, Vol. 35, No. 6, 1997, pp. 990–999; also AIAA Paper 96-0320, Jan. 1996.

[9] Meier, H. U., and Kreplin, H. P., "Experimental Investigation of the Boundary Layer Transition and Separation on a Body of Revolution," *Zeitschrift fuer Flugwissenschaft und Weltraumforschung*, Vol. 4, No. 2, 1980, pp. 65–71.

[10] Squire, L. C., "The Motion of a Thin Oil Sheet Under the Boundary Layer on a Body," *Journal of Fluid Mechanics*, Vol. 11, Pt. 2, 1960, pp. 161–179.

[11] Chesnakas, C. J., and Simpson, R. L., "An Investigation of the Three-Dimensional Turbulent Flow in the Crossflow Separation Region of a 6:1 Prolate Spheroid," *Experiments in Fluids*, Vol. 17, 1994, pp. 68–74.

[12] Wetzel, T. G., "Unsteady Flow Over a 6:1 Prolate Spheroid," Ph.D. Dissertation, Dept. of Aerospace and Ocean Engineering, Virginia Polytechnic Inst. and State Univ., Rept. API-AOE-232, Blacksburg, VA, March 1996; distributed by DTIC, No. ADA3071412XSP, Fort Belvoir, MD, 1996.

[13]Townsend, A. A., *Structure of Turbulent Shear Flow*, 2nd ed., Cambridge Univ. Press, New York, 1976, p. 43.

[14]Poll, D. I. A., "On the Effects of Boundary Layer Transition on a Cylindrical Afterbody at Incidence in Low-Speed Flow," *Aeronautical Journal*, Vol. 89, Oct. 1985, pp. 315–327.

[15]Hall, R. M., "Influence of Reynolds Numbers on Forebody Side Forces for 3.5-Diameter Tangent-Ogive Bodies," AIAA Paper 87-2274, Aug. 1987.

[16]Chang, M. S., and Purtell, L. P., "Three-Dimensional Flow Separation and the Effect of Appendages," *16th Symposium on Naval Hydrodynamics*, National Academy Press, Berkeley, CA, 1986, pp. 352–370.

[17]Tinker, S. J., "Numerical Simulation of Separated Flow over Bodies of Revolution," Admiralty Research Establishment, Rept. AMTE(H) R85209, Haslar, Gosport, England, UK, 1985.

[18]Goody, M., Simpson, R. L., and Chesnakas, C. J., "Surface Pressure Fluctuations and Pressure Velocity Correlations Produced by a Separated Flow Around a Prolate Spheroid at Incidence," AIAA Paper 97-0485, Jan. 1997.

[19]Ahn, S., and Simpson, R. L., "Crossflow Separation on a Prolate Spheroid at Angles of Attack," AIAA Paper 92-0428, Jan. 1992.

A. Plotkin
Associate Editor